



Available online at <https://ganitjournal.bdmathsociety.org/>

## GANIT: Journal of Bangladesh Mathematical Society

**GANIT** *J. Bangladesh Math. Soc.* 45.2 (2025) 066–082

DOI: <https://doi.org/10.3329/ganit.v45i2.86703>



# An Evolving Game Simulating Approach to Perceive the Aptness of Quarantine and Social Distancing Policy to Mitigate Contagious Disease Transmission

Zarin Tusnim<sup>1,2\*</sup> and Muntasir Alam <sup>\*1</sup>

<sup>1</sup> Department of Applied Mathematics, University of Dhaka, Bangladesh

<sup>2\*</sup> Department of Computer Science and Engineering, Daffodil International University, Bangladesh

## ABSTRACT

We concentrate on the suppression of infectious diseases that give rise to temporary or imperfect immunity. It introduces a stochastic SVEIR model with vaccinated (V) and exposed (E) populations, and incorporates quarantine and isolation (i.e., social distancing) as the two principal control strategies. The model is defined on non-spatial networks and includes two parameters — the latent carrier rate ( $\rho$ ) and the rate of conveying ( $\mu$ ) to characterise transmission behaviour in more realistic terms. This paper assesses the synergy between vaccination, isolation and quarantine policies, accounting for both voluntary and imposed behaviors as well as for the resource costs of interventions. The aim is to decide on the best vaccination strategy to achieve elimination. The strategy considers both proactive (e.g., vaccination) and reactive (e.g., isolation/quarantine) measures if we want to minimize the impact of pandemic. This joint control approach is based on a mean field theory based on the SVEIR model.

© 2025 Published by Bangladesh Mathematical Society

**Received:** November 22, 2025 **Accepted:** December 18, 2025 **Published Online:** December 30, 2025

**Keywords:** Quarantine; Isolation; Vaccination; Infectious diseases; SVEIR model.

**AMS Subject Classifications 2025:** 11A41.

## 1 Introduction

A pandemic of infectious disease involves a multi-faceted response, including vaccination, quarantine, isolation, and other preventive measures [1]. These measures are necessary for controlling the spread of infections and public health protection. In this section, we analyze the multi-faceted relationships between these intervention approaches. In particular, we include two important parameters: Its parameters are:  $\rho$  (latent carrier rate) and  $\mu$  (carrying rate) [2]. The enactment and feasibility of public health interventions is frequently dependent on the costs associated with interventions, therefore it is of utmost importance to develop of an understanding of the relationship between expenditure and its influence on individual and societal welfare. To study decision-making [3] dynamics in such an environment, we use the well-established method known as Evolutionary Game Theory (EGT) [4] to model the strategic interplays between agents.

\*Corresponding author. Email address : [muntasir.appmath@du.ac.bd](mailto:muntasir.appmath@du.ac.bd)

Using EGT [4], we explore the impact of the costs of a vaccine on the willingness of individuals to vaccinate, and how this then affects the patterns of transmission of disease. In epidemic and pandemic situations, quarantine laws are significantly crucial in controlling the disease spread process [5]. We make similar analysis for the assessment of the costs of being in quarantine off the EGT [6, 7]. In our model we introduce two important parameters :  $\rho$  and  $\mu$ . The parameter  $\rho$  characterizes the latent carrier rate, that is, the original number of population who are contaminated with a contagious disease, but remain asymptomatic. These infected individuals are especially critical in public health efforts, because as soon as they are diagnosed, they can be isolated, inform all of their contacts and potentially notify the community early, all of which are crucial to limit further spread of a disease [8–10].

The parameter  $\mu$  indicates the reduction in infectiousness due to isolation, indicating the decreased probability of disease transmission when infected individuals are separated from the general population. Isolation serves as a targeted public health measure to limit exposure and mitigate the overall risk of epidemic escalation.

Vaccination [11] is an enormously productive way to halt and combat infectious illness, with successes such as the eradication of smallpox and major reductions in infantile illnesses such as whooping cough and measles. In some diseases and with some vaccines, immunity can be long-lasting or even need booster shots [12]. Quarantine and isolation are other forms of public health interventions to control disease transmission, particularly during infectious disease outbreaks such as SARS outbreak [13–15]. Although isolation [16] is well accepted, quarantine [16] has ethical implications as it exposes healthy people to risk of infection [17]. Both strategies are intended to minimize interactions between individuals who can infect one another [18]. But it's unclear how much of a role each one plays in driving outbreaks. The study takes quarantine and isolation to be uniformly imposed, regardless of voluntary action as modeled through Evolutionary Game Theory (EGT).

The former highlights the interplay of behavioral dynamics and epidemic control, weaving voluntary with coercive policies in an evolutionary game-theoretic SEIR model to investigate how per capita out-of-pocket cost for vaccination as well as policy cost, affect economically induced vaccination uptake and quarantine adherence. The former focuses on strategic action and compliance with policy. We study vaccination behaviour by embedding imitation and aspiration dynamics within a mean-field model. It focuses on how people make a decision to be vaccinated with one of the two alternative vaccines under different cost, efficacy, expectation and timing (early vs. delayed) situations. It focuses on behavioral strategy and social dilemma with updating process for the final vaccination coverage. Using a game-theoretical SVIR model, the first paragraph studies multi-strain epidemics concerning strategic vaccine uptake, imitation dynamics, behavioural changes and the relative efficacy of two vaccines for respectively primary strain and mutant strains. Both the stochastic and fuzzy models express uncertainty, but they belong to different types of uncertainty. Stochastic models utilize randomness to account for uncertainty, and events (such as infection and recovery) occur according to probability distributions. On the other hand, in a fuzzy theoretical system uncertainty is described by imprecision or vagueness of parameter values with respect to some kind; that is, fuzzy numbers representing vague data or data appearing not clearly defined are employed. For instance, the parameters of transmission or vaccination rates in fuzzy SVEIR models are considered as TFNs to incorporate vagueness. In the present work we address parameter vagueness in an SVEIR model with a view to estimating disease spread randomness [19–22].

## 2 Model Visualization by Using Technique

A typical epidemic persists until only one infected individual remains. During this period, population fractions—such as vaccinated, quarantined, and isolated individuals—remain constant, as births and deaths are excluded from the model [23, 24]. The optional vaccination strategy assumes individuals can choose to re-vaccinate each season [25, 26]. Our dynamic evolutionary model includes two phases: a pre-epidemic stage where individuals decide on vaccination based on cost and risk, and a pandemic phase where unvaccinated individuals risk infection. To capture transmission fluctuations, we use a stochastic model incorporating quarantine and isolation [27–29].

### 2.1 Building the Preferred Model

The model we suggest consists of an SVEIR model, which stands for Susceptible, Vaccinated, Exposed, Infected, Recovered, assuming lifelong immunity [30]. It adds other slots to account for quarantine and isolation, and these two slots are merged into a mixed compartment (C) for individuals subjected to any of those interventions or both. The population is considered to be infinitely large, well-mixed, and not geographically structured [31].

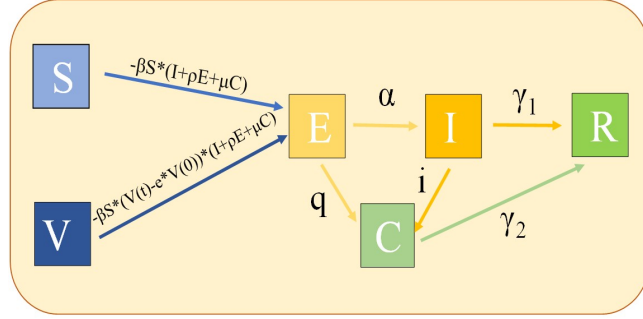


Figure 2.1: A schematic illustration of the preferred model.

Two important parameters are brought in: latent carrier rate ( $\rho$ ), which is the infected but asymptomatic are infectious, and conveying rate ( $\mu$ ), defined as the number of infected others will be reduced by quarantine. One may become susceptible (S) in contact with the infected (I), be exposed  $\alpha$  with a rate of disease progression by the rate of transmission  $\beta$ . Exposed can switch to quarantine (C) at rate  $q$ , or become infected (I), whereas a portion of the contaminated can be isolated (C) at rate  $i$ . Infectives recover at rates  $\gamma_1(I)$  and  $\gamma_2(C)$ , respectively.

Vaccination is viewed as optional and imperfect. The vaccine-induced efficacy,  $e$  ( $0 \leq e \leq 1$ ) [32–34], is defined as the portion of immune individuals after being vaccinated. One share ( $1 - e$ ) can be left vulnerable. Moreover, immunity might decrease with time and reinfection might occur.

The model differentiates active (vaccination) and passive (quarantine and isolation) interventions. Significantly, not all exposed cases develop the disease, and being quarantined on detection. The basic replication number is given by

$$R_0 = \frac{\beta}{\gamma} \quad (2.1)$$

, indicating the mean number of minor contaminations created by a contagious individual in an entirely susceptible people.

## 2.2 Configuration of the Preferred Model

The stochastic SIR model, a mainstay of epidemic models, was first discussed in the seminal paper of McKendrick and Kermack [11]. In the model, susceptibles are healthy, but have a possibility of getting infected when in contact with infectives. Quarantine and isolation are passive measures whereas vaccination is an active component of disease prevention. However, due to the narrow scope of these measures, vaccinated and self-quarantined individuals may still be at risk of exposure [35–37].

In the dynamical model under proposed, six different compartments ( $S(tm)$ ,  $V(tm)$ ,  $E(tm)$ ,  $I(tm)$ ,  $C(tm)$ ,  $R(tm)$ ) are considered with  $S(tm)$ ,  $V(tm)$ ,  $E(tm)$ ,  $I(tm)$ ,  $C(tm)$ , and  $R(tm)$  being the notations of susceptible, vaccinated, exposed, infected, combined (quarantine/isolation) [38], and recovered individuals at time  $tm$ . All fractions must add to 1:

$$S(tm) + V(tm) + E(tm) + I(tm) + C(tm) + R(tm) = 1 \quad [16].$$

The initial fraction of immune population is  $V(0)$  and  $e \cdot V(0)$  is effectively protected. The difference  $V(t) - e \cdot V(0)$  may depend on the disease strain. The model dynamics are governed by a set of nonlinear ODEs, which include all preventive measures.

$$\frac{dS(z, tm)}{dtm} = -\beta \cdot S(z, tm) \cdot (I(z, tm) + \rho \cdot E(z, tm) + \mu \cdot C(z, tm)) \quad (1.1)$$

$$\frac{dV(z, tm)}{dtm} = -\beta \cdot (V(z, tm) - e \cdot V(z, 0)) \cdot (I(z, tm) + \rho \cdot E(z, tm) + \mu \cdot C(z, tm)) \quad (1.2)$$

$$\begin{aligned} \frac{dE(z, tm)}{dtm} = & \beta \cdot S(z, tm) \cdot (I(z, tm) + \rho \cdot E(z, tm) + \mu \cdot C(z, tm)) \\ & + \beta \cdot (V(z, tm) - e \cdot V(z, 0)) \cdot (I(z, tm) + \rho \cdot E(z, tm) + \mu \cdot C(z, tm)) \\ & - \alpha \cdot E(z, tm) - q \cdot E(z, tm) \end{aligned} \quad (1.3)$$

$$\frac{dI(z, tm)}{dtm} = \alpha \cdot E(z, tm) - i \cdot I(z, tm) - \gamma \cdot I(z, tm) \quad (1.4)$$

$$\frac{dC(z, tm)}{dtm} = q \cdot E(z, tm) + i \cdot I(z, tm) - \delta \cdot C(z, tm) \quad (1.5)$$

$$\frac{dR(z, tm)}{dtm} = \gamma \cdot I(z, tm) + \delta \cdot C(z, tm) \quad (1.6)$$

The following are the starting circumstances for a set of equations (1.1) to (1.6) :

$$S(0) = 1 - z \geq 0, \quad V(0) = z \geq 0, \quad E(0) \geq 0, \quad I(0) \geq 0, \quad J(0) \geq 0, \quad R(0) \geq 0 \quad (1.7)$$

We note that Equations (1.1)–(1.6) and the initial condition (1.7) are defined on  $[0, +\infty)$  and stay positive at every moment of time  $tm \geq 0$ . All the variables  $\alpha, \beta, \gamma, \delta, \rho, \mu$  are positive.

At the beginning of the pandemic,  $z$  and  $1 - z$  are the elementary kinds of people 1: give them the proportions of vaccinated and susceptibles. The model provides a solid mathematic foundation for pandemic dynamics. Here,  $\alpha$  is the progression rate, and  $\beta$  the conveyance rate,  $\gamma$  the recovery rate,  $\delta$  the revised recovery rate,  $\rho$  is the latent carrier rate, and  $\mu$  is the transmission from the isolated individuals.

### 2.3 Game-Theoretic Categorization of Individuals

A game-theoretic method used to divide individuals into four groups according to their health status and the total cost (Table 2.1).

State/Strategy	Fit	Contaminated
Immunized (I)	FI	CI
Non-Immunized (NI)	SFR	FFR

Table 2.1: Four categories of individual strategies in a pandemic scenario.

- **FI (Fit Immunizer):** Vaccinates and remains healthy.
- **CI (Contaminated Immunizer):** Vaccinates and become ill after infection.
- **SFR (Successful Free-Rider):** Whoever is not vaccinated and stays healthy due to herd immunity.
- **FFR (Failed Free-Rider):** Not vaccinated and becomes infected, pays for illness.

### 2.4 Payoff Structure Evolution in Games

Payoff-Based Strategy Dynamics : Vaccine-preventable disease not only makes people sick, it can also cause long-term effects or death, resulting in hospitalization, doctor's visits, time away from work and school, and other negative impacts to society in terms of cost and health. A pandemic season terminates when everyone enters  $R$  because individuals can now rethink their strategies by performing a payoff analysis.

The relative charge of inoculation is given by:

$$C_{Re} = \frac{C_i}{C_c}, \quad (0 \leq C_{Re} \leq 1)$$

where  $C_i$  is the charge of immunization and  $C_c$  is the charge of contamination.

According to strategy and health condition, each people is organized in one of four different payoff types (Table 2.2).

State/Strategy	Fit	Contaminated
Immunized (I)	$-C_{Re}$	$-C_{Re} - 1$
Non-Immunized (NI)	0	-1

Table 2.2: Projected payoff structure after each pandemic season.

Vaccination choices are made construct on trade-offs between the cost of defense and the threat of contamination or quarantine. These are dynamic decisions based on pandemic prevalence. Average total payoffs are calculated for every strategy change as:

$$\langle \pi \rangle, \quad \langle \pi_I \rangle, \quad \langle \pi_{NI} \rangle$$

representing the average social, vaccinated, and non-vaccinated payoffs respectively.

$$\langle \pi \rangle = -C_{\text{Re}} \cdot FI(z, \infty) - (C_{\text{Re}} + 1) \cdot CI(z, \infty) - FFR(z, \infty) \quad (1.8)$$

$$\langle \pi_I \rangle = \frac{-C_{\text{Re}} \cdot FI(z, \infty) - (C_{\text{Re}} + 1) \cdot CI(z, \infty)}{z} \quad (1.9)$$

$$\langle \pi_{NI} \rangle = \frac{-FFR(z, \infty)}{1 - z} \quad (1.10)$$

## 2.5 Strategy Modernizing

This model compares strategies effectiveness according to Game Theory, assuming individuals make rational decisions [39]. After each pandemic season, people again review their choices in light of the previous payoffs and decide whether to stick or switch [40–42]. The fundamental mechanism of the inoculation game is set-on by the payoff in the last season. Alongside the different methods of update- Individual-Situated Risk Analysis (IS-RA), Strategy-Situated Risk Analysis (SS-RA) and Staright Commitment (SC), we chose the IS-RA modernization rule in the model. We adopt the IS-RA modernization rule in the model [43].

### 2.5.1 Individual-Situated Risk Analysis (IS-RA) modernization rule

Pair-wise Fermi [39] modernization is a popular model on strategy modernization. In that model, one agent selects randomly another agent copying his/her strategy with a given probability relying on the contrast of the payoffs [23], where is the probability of adoption:

$$P(S_i \leftarrow S_j) = \frac{1}{1 + \exp\left[-\frac{\pi_j - \pi_i}{k}\right]}$$

Here,  $k$  ( $> 0$ ) is the intensity of selection, where the lower the value of  $k$ , the more sensitivity for payoff differences. We adopt ( $k = 0.1$ ) in our study as also used in previous literature with the IS-RA rule we have the following transition probabilities:

$$\begin{aligned} P(FI \leftarrow SFR) &= \frac{1}{1 + \exp\left[-\frac{0+C_{\text{Re}}}{k}\right]} \\ P(FI \leftarrow FFR) &= \frac{1}{1 + \exp\left[-\frac{-1+C_{\text{Re}}}{k}\right]} \\ P(CI \leftarrow SFR) &= \frac{1}{1 + \exp\left[-\frac{0+C_{\text{Re}}+1}{k}\right]} \\ P(CI \leftarrow FFR) &= \frac{1}{1 + \exp\left[-\frac{-1+C_{\text{Re}}+1}{k}\right]} \\ P(SFR \leftarrow FI) &= \frac{1}{1 + \exp\left[-\frac{C_{\text{Re}}+0}{k}\right]} \\ P(SFR \leftarrow CI) &= \frac{1}{1 + \exp\left[-\frac{-C_{\text{Re}}-1-0}{k}\right]} \\ P(FFR \leftarrow FI) &= \frac{1}{1 + \exp\left[-\frac{C_{\text{Re}}-1}{k}\right]} \\ P(FFR \leftarrow CI) &= \frac{1}{1 + \exp\left[-\frac{C_{\text{Re}}+1-1}{k}\right]} \end{aligned}$$

Here, we show that an IS-RA and an SS-RA give rise to different dynamical behavior, though we will limit our attention here to the IS-RA [16].

### 2.5.2 Dynamics of Evolution

At the end of each season, post-pandemic, people can adapt their strategies along the lines of previous observations, with or without immunization, thus masking the dynamics of vaccine coverage ( $z$ ) over time. According to the IS-RA strategy modernizing rule, the time evolution of ( $z$ ) reads:

$$\begin{aligned} \frac{dz}{dtm} = & FI(z, \infty) \cdot SFR(z, \infty) \cdot [P(SFR \leftarrow FI) - P(FI \leftarrow SFR)] \\ & + FI(z, \infty) \cdot FFR(z, \infty) \cdot [P(FFR \leftarrow FI) - P(FI \leftarrow FFR)] \\ & + SFR(z, \infty) \cdot CI(z, \infty) \cdot [P(SFR \leftarrow CI) - P(CI \leftarrow SFR)] \\ & + CI(z, \infty) \cdot FFR(z, \infty) \cdot [P(FFR \leftarrow CI) - P(CI \leftarrow FFR)] \end{aligned} \quad (1.20)$$

## 3 Result and Discussion

In this part of the paper Evolutionary Game Theory (EGT) [16] is being investigated using time series and phase plane analysis for the analysis of the population dynamics. Our attention is given to understanding how the evolution of strategies in a population is influenced by parameters like vaccine's efficacy, vaccine cost, quarantine rate, recovery rate, and rate of progression.

Time series analysis is carried out in MATLAB the observed population dynamics qualitatively change by changing parameters such as the payoff values and the initial distributions of strategies. For phase plane analysis, C++ and Python allow visualization of 2D dynamics and the monitoring of strategic shifts across time.

EGT enables us to consider how strategies fare in interaction with each other and how widespread and successful strategies spread, and helps to uncover patterns of cooperation, competition, and social interaction. This section includes: Section 3.1: Time series analysis techniques and interpretations Section 3.2: Phase plane method, Construction of the 2D heat map, and Results interpretation.

### 3.1 Time Series Evaluation for a Single Season

This section examines the epidemic dynamics decoupled from game-theoretic considerations. With an initial vaccination coverage of 46% ( $V(0) = 0.46$ ), and initially very small proportions of exposed individuals ( $E(0) = 0.003$ ), infected ( $I(0) = 0.0006$ ) and combined (isolation and quarantine) individuals ( $C(0) = 0.0004$ ), the disease spreads, peaks, and is eventually cleared within one pandemic season.

We test the robustness of the model through time-series analysis and an equilibrium sensitivity analysis. The variables utilized are:  $\beta = 0.833$ ,  $\gamma = 0.33$ ,  $\delta = 0.38$ ,  $\alpha = 0.20$ ,  $\rho = 0.7$ ,  $\mu = 0.5$ ,  $q = 0.6$ ,  $i = 0.4$ ,  $e = 0.6$ .

where ( $q$ ) and ( $i$ ) are the quarantine and isolation pick-up rates, and ( $\rho$ ) and ( $\mu$ ) are the latent carrier and conveying rates, respectively.

We consider four different policies, namely no intervention, isolation, quarantine, and a combined policy. From figs.3.2-3.4, we see that the coupled policy is the most efficient in terms of suppressing infection. Recovery goes up as susceptibility goes down, but vaccines are not perfect. The highest levels of infection are associated with no policy and the lowest with combined policies. We chose these values based on a realistic epidemic scenario with infection onset, peak, and wane in a season. The initial conditions represent a not-widely-vaccinated population and very few cases, typical of early times in the pandemic. Rates including transmission and recovery, latent, and conveying rates were parameterized based on biologically reasonable bounds to graduate meaningful epidemic of dynamics. The quarantine and isolation pick-up rates were chosen as examples of intermediate public health responses. Collectively, these parameters enable the framework to attain equilibrium and establish an appropriate standrad for sensitivity analysis and future game theoretic expansions.

### 3.2 Phase-Plane Evaluation Employing 2D Heat Diagrams

Employing the standard SVEIR epidemic framework, we utilize an evolutionary game-theoretic model over multiple seasons to quantify the impact of voluntary vaccination under different parameters. This approach fuses isolation-quarantine measures (joint) and the 2D phase heat maps (in Fig. 8) of the epidemic to demonstrate systems behaviour and their equilibrium state. The study investigates the social burden of the cost of inoculation and the effectiveness of inoculation by blending the epidemic dynamics and the feedback strategy of the public

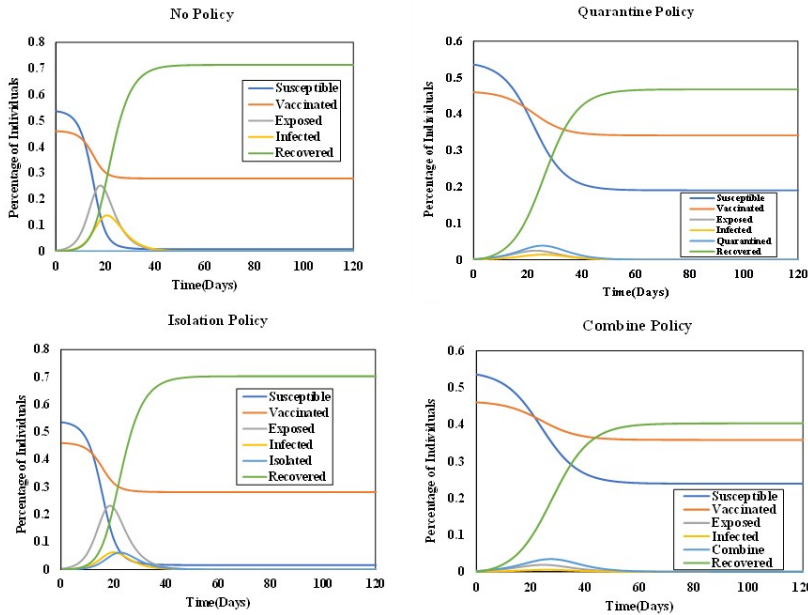


Figure 3.1: *Time evolution line charts comparing four policy scenarios: no policy, quarantine, isolation, and combined policy. Variables utilized are  $\beta = 0.8333$ ,  $\gamma = 0.3333$ ,  $\delta = 0.38$ ,  $\alpha = 0.20$ ,  $\rho = 0.7$ ,  $\mu = 0.5$ ,  $e = 0.6$ . Policy-specific values are set like : no policy ( $q = 0.0$ ,  $i = 0.0$ ), quarantine ( $q = 0.6$ ,  $i = 0.0$ ), isolation ( $q = 0.0$ ,  $i = 0.4$ ), and combined ( $q = 0.6$ ,  $i = 0.4$ ). Exposure and infection are the greatest under no policy with combined policy having the lowest both.*

on the disease incidence. We consider three evolutionary end-points — Final Epidemic Size (FES), Portion of Vaccinated People (VC), and Average Social Payoff (ASP). FES represents the aggregate immune population, VC represents the vaccination fraction and ASP represents the average social payoff.

We explore policy effects by varying the quarantine and isolation pick-up rates ( $q$  and  $i$ ), as well as parameters  $\rho$  (latent infectiousness) and  $\mu$  (reduction in infectiousness due to the isolation). We present three panels in each section (a, b, c) with comparisons of the resulting outcome on pre-emptive vaccination under various 8 parameter settings:  $\alpha = 0.30, 0.40$ ,  $\delta = 0.45, 0.55$ ,  $\rho = 0.2, 0.5$ , and  $\mu = 0.3, 0.6$ . Results are obtained using the IB-RA strategy updating scheme.

In Figs.8 - 10, disease free (dark blue) to epidemic (dark red) weighted transitions are shown. These color maps show the influence of the vaccine price and protection rate on the FES, VC and ASP for  $R_0 = \frac{\beta}{\gamma} = 2.5$ . At a lower vaccine efficacy and higher costs, free-riding behavior prevails, resulting in widespread outbreaks despite interventions.

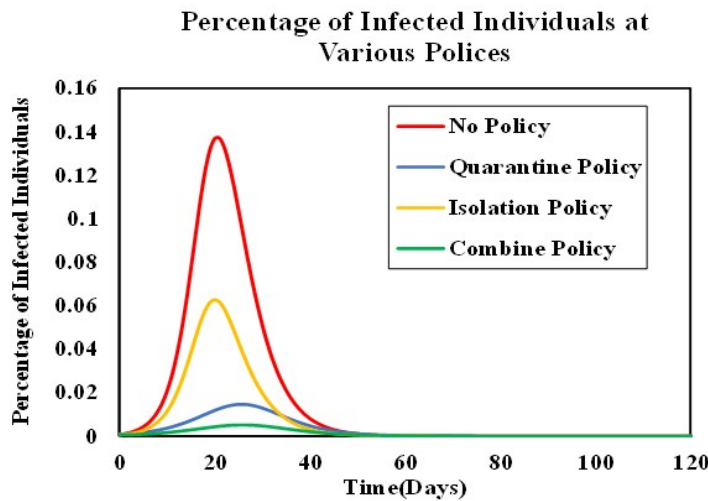


Figure 3.2: Under for different strategies, the infected proportion trajectories are determined by the rates of quarantine ( $q$ ) and isolation ( $i$ ). The parameter set includes  $\beta = 0.8333$ ,  $\gamma = 0.3333$ ,  $\delta = 0.38$ ,  $\alpha = 0.20$ ,  $\rho = 0.7$ ,  $\mu = 0.5$ ,  $q = 0.6$ ,  $i = 0.4$ , and vaccine effectiveness  $e = 0.6$ . We generate the figure using the following scenarios: no policy ( $q = 0$ ,  $i = 0$ ), quarantine policy ( $q = 0.6$ ,  $i = 0$ ), isolation policy ( $q = 0$ ,  $i = 0.4$ ), and combined policy ( $q = 0.6$ ,  $i = 0.4$ ). No policy has the highest peak infection (0.14), followed by isolation (0.06), quarantine (0.01) and combined policy has the lowest peak infection (0.0001). Quarantine is superior to simple isolation, and the combination of both is the best for minimizing disease spread.

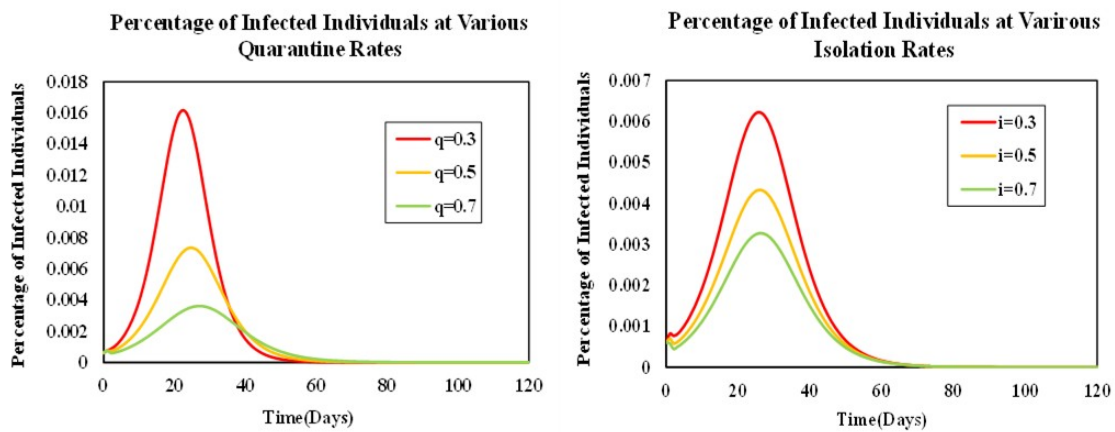


Figure 3.3: The infection rate is demonstrated to vary seasonally due to different degrees of isolation and quarantine. In the first case, isolation is fixed at 0.4 and quarantine varies in the set (0.3, 0.5, 0.7) while in the second, quarantine is fixed at 0.6 and isolation varies in the same manner. We found that the increase in quarantining or isolation reduces the time to get to the apex infection, and the elevated value of  $c$ , the quicker the infection is contained by mixing the isolating or quarantining population.

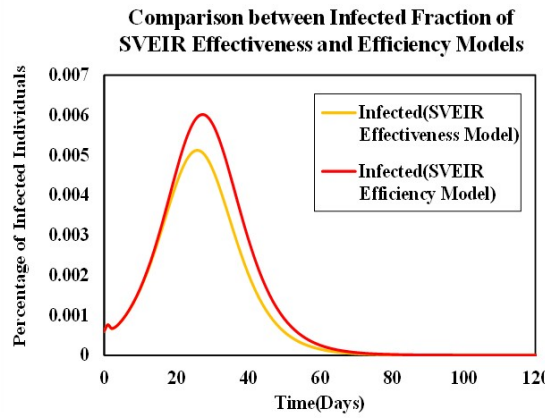


Figure 3.4: The comparison of the SVEIR effectiveness and efficiency models indicates that the effectiveness model predicts the final infected fraction to be slightly less than 0.005 compared to the efficiency model (0.006), even though both models begin with  $I(0) = 0.0006$ . All the above graphs were developed using SVEIR effectiveness model.

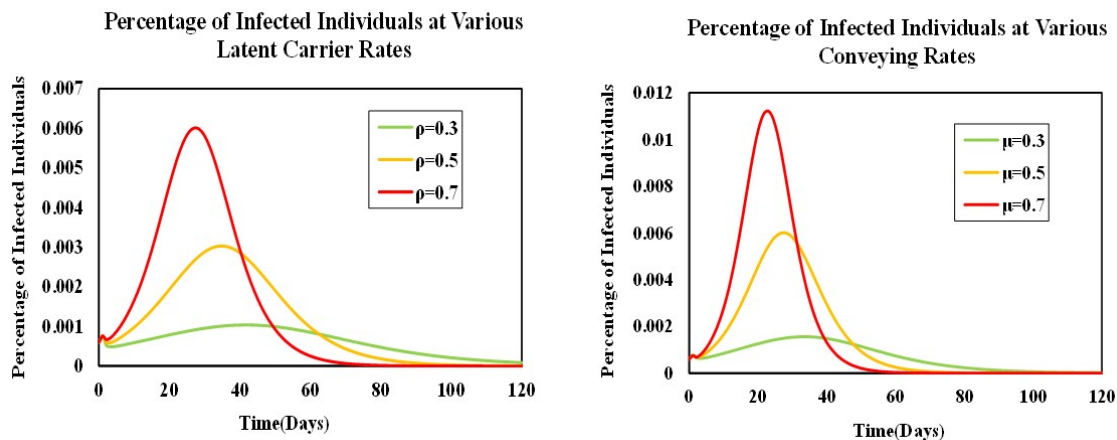


Figure 3.5: This graph shows the impact of variation of latent carrier rate ( $\rho$ ) and conveying rate ( $\mu$ ) on infected fraction. When  $\mu = 0.5$ , rampant spread of infections occurs more quickly with higher  $\rho$  values (0.3, 0.5, 0.7). Likewise, for  $\rho = 0.7$ , a larger  $\mu$  leads to a more extensive infection spread. E.g., at  $\rho = 0.7$ , the number of infections is of order 0.005, while at  $\rho = 0.3$  it is less than 0.001. Therefore, a higher  $\rho$  and  $\mu$  contribute to higher infections and the importance of a quarantine and isolation.

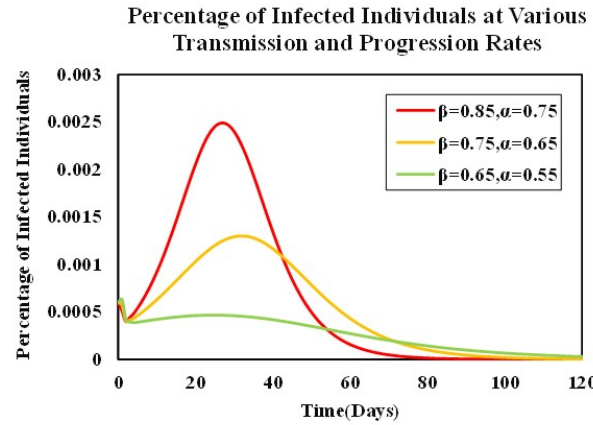


Figure 3.6: It illustrates how the rate of transmission and the rate of progression of the disease affect epidemic resurgence. Dynamic simulations with different transmission rates (and recovery rate) illustrate that a higher transition or progression factor leads to a larger infected fraction. For example, at transmission rate of 0.85 and progression rate of 0.75 the peak of the infection is about 0.0025. Smaller transmission rates result in smaller infected proportions—demonstrating the influence factor of transmission rather than of the initial infection proportion.

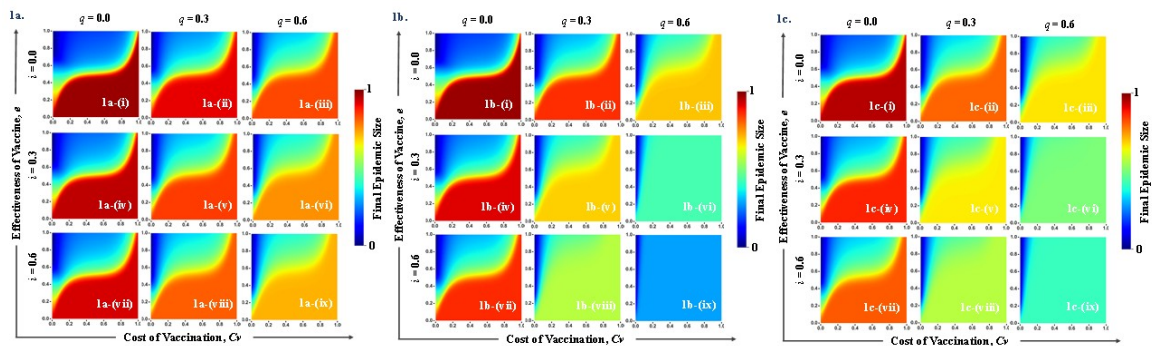


Figure 3.7: Final Epidemic Size (FES) for distinct values of inoculation costs and effectiveness. Scenarios: **1a**–**1c** represent different parameter settings: **1a**:  $\delta = 0.45$ ,  $\alpha = 0.40$ ,  $\rho = 0.5$ ,  $\mu = 0.6$ ; **1b**:  $\delta = 0.55$ ,  $\alpha = 0.40$ ,  $\rho = 0.5$ ,  $\mu = 0.3$ ; **1c**:  $\delta = 0.55$ ,  $\alpha = 0.30$ ,  $\rho = 0.2$ ,  $\mu = 0.6$ , with fixed  $\beta = 0.8333$ ,  $\gamma = 0.3333$ . Pickup rates for quarantine ( $q$ ) and isolation ( $i$ ) are varied as  $q, i \in \{0.0, 0.3, 0.6\}$ . Lower vaccine cost and higher efficacy decrease the FES according to the findings. Epidemic spread is reduced with higher recovery rate ( $\delta$ ) but increased as progression ( $\alpha$ ), latent carrier ( $\rho$ ), and conveying rates ( $\mu$ ) increase further. Larger  $q$  and/or  $i$  tilt the result toward blue which is lower FES and smaller  $q$  and/or  $i$  enhance the pandemic intensity (red). Policies to quarantine seem to be more efficient than isolation to control outbreaks.

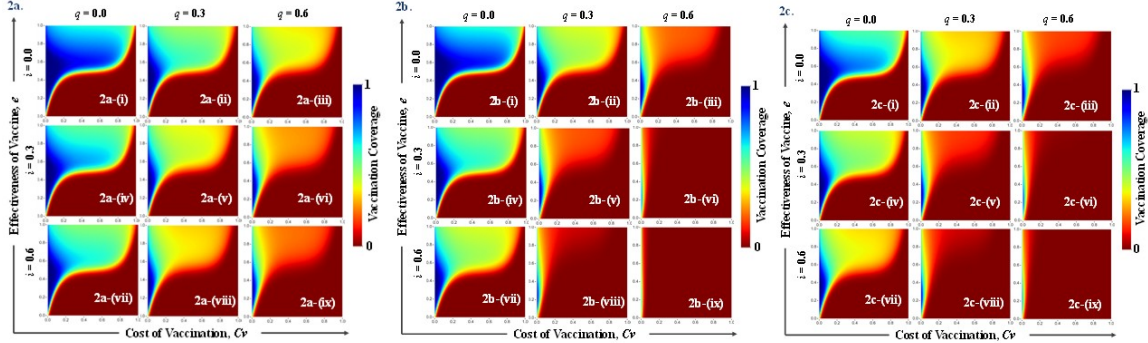


Figure 3.8: Vaccination Coverage (VC) for distinct values of inoculation costs and effectiveness. Scenarios: 2a–2c reflect varying parameters: 2a:  $\delta = 0.45$ ,  $\alpha = 0.40$ ,  $\rho = 0.5$ ,  $\mu = 0.6$ ; 2b:  $\delta = 0.55$ ,  $\alpha = 0.40$ ,  $\rho = 0.5$ ,  $\mu = 0.3$ ; 2c:  $\delta = 0.55$ ,  $\alpha = 0.30$ ,  $\rho = 0.2$ ,  $\mu = 0.6$ , with fixed  $\beta = 0.8333$ ,  $\gamma = 0.3333$ . Quarantine ( $q$ ) and isolation ( $i$ ) pickup rates vary over  $\{0.0, 0.3, 0.6\}$ . The results reveal that VC is less in the cases of high-cost vaccines with low efficacy (red zones), but higher in the cases of low-cost vaccines with high efficacy (blue zones). Effective quarantine isolation can contain outbreaks even with limited vaccination. Therefore strong public health policies addressing affordability, awareness and confinement practices are important to encourage optimal vaccination behaviour.

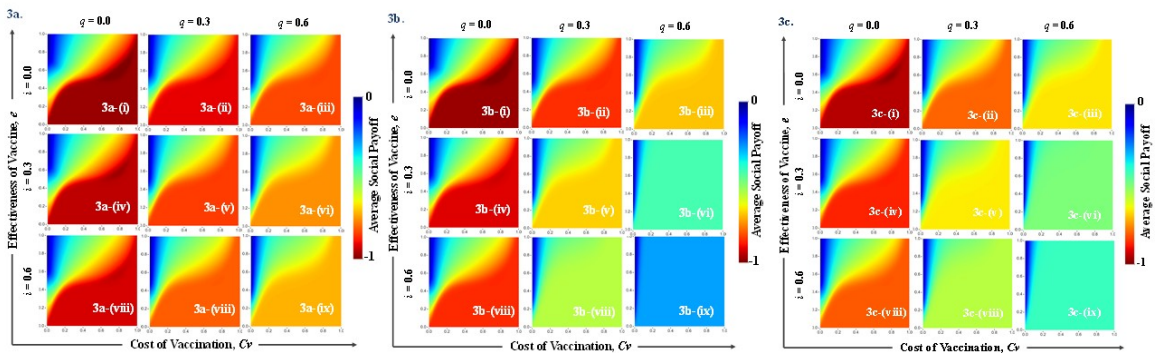


Figure 3.9: Average Social Payoff (ASP) for distinct values of inoculation costs and effectiveness. Scenarios: 3a:  $\delta = 0.45$ ,  $\alpha = 0.40$ ,  $\rho = 0.5$ ,  $\mu = 0.6$ ; 3b:  $\delta = 0.55$ ,  $\alpha = 0.40$ ,  $\rho = 0.5$ ,  $\mu = 0.3$ ; 3c:  $\delta = 0.55$ ,  $\alpha = 0.30$ ,  $\rho = 0.2$ ,  $\mu = 0.6$ , with  $\beta = 0.8333$ ,  $\gamma = 0.3333$  constant. Pickup rates  $q = \{0.0, 0.3, 0.6\}$  (quarantine) and  $i = \{0.0, 0.3, 0.6\}$  (isolation) are varied. Results shows that increased vaccine coverage and effectiveness lead to high ASP, and blue zones drive low intervention rates. Small changes in epidemic outcomes and vaccine uptake have significant consequences on ASP, emphasizing the importance of combining vaccination with interventions that are highly effective quarantine-isolation-based.

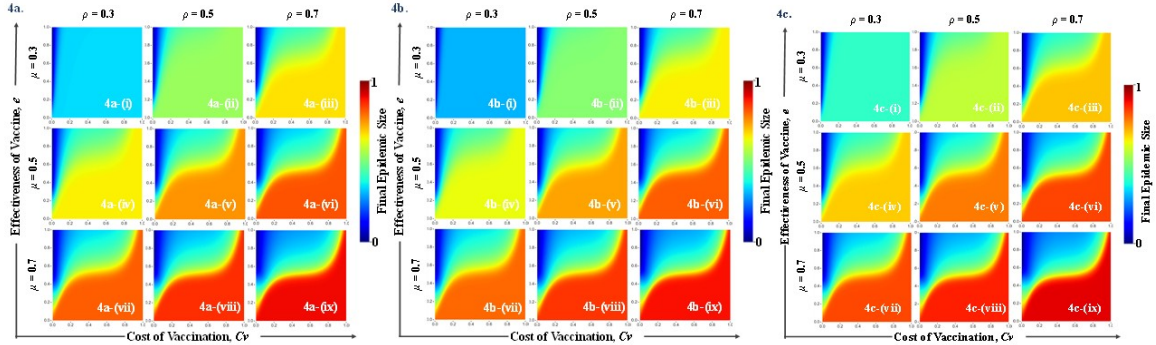


Figure 3.10: Final Epidemic Size (FES) for distinct values of inoculation costs and effectiveness. Scenarios: 4a:  $\gamma = 0.18517$  ( $R_0 = 4.5$ ), 4b:  $\gamma = 0.27777$  ( $R_0 = 3.0$ ), 4c:  $\gamma = 0.33333$  ( $R_0 = 2.5$ ), with fixed parameters  $\beta = 0.8333$ ,  $\delta = 0.38$ ,  $\alpha = 0.20$ ,  $q = 0.6$ , and  $i = 0.4$ . Latent carrier rate  $\rho = \{0.3, 0.5, 0.7\}$  and conveying rate  $\mu = \{0.3, 0.5, 0.7\}$  are varied. Higher  $\rho$  and  $\mu$  lead to more FES, and the red areas represent a fast extension of the illness. On the contrary, the combined isolation-quarantine policies lead to a significant reduction of FES, which verifies the effectiveness of combined isolation-quarantine policies in restraining disease outbreak.

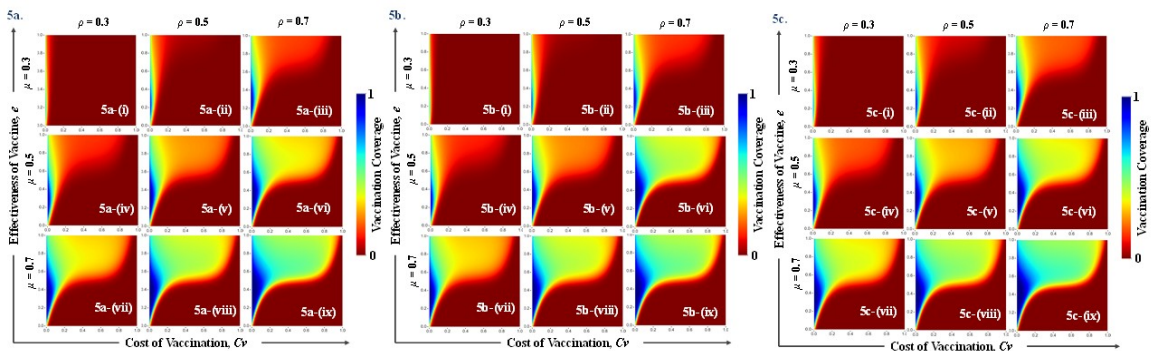


Figure 3.11: Vaccination Coverage (VC) for distinct values of inoculation costs and effectiveness. Scenarios: 5a:  $\gamma = 0.18517$  ( $R_0 = 4.5$ ), 5b:  $\gamma = 0.27777$  ( $R_0 = 3.0$ ), 5c:  $\gamma = 0.33333$  ( $R_0 = 2.5$ ). Fixed parameters:  $\beta = 0.8333$ ,  $\delta = 0.38$ ,  $\alpha = 0.20$ ,  $q = 0.6$ ,  $i = 0.4$ . Latent carrier rate  $\rho = 0.3, 0.5, 0.7$  and conveying rate  $\mu = 0.3, 0.5, 0.7$  are varied. Results reveal that the VC increases when  $\rho$  and  $\mu$  increase, which means individuals tend to get more shots as perceived risk raises. But uptake declines if the cost of the vaccine is too high. It is therefore necessary that, alongside vaccination, strict isolation and quarantine measures are in place to prevent contact with infected individuals.

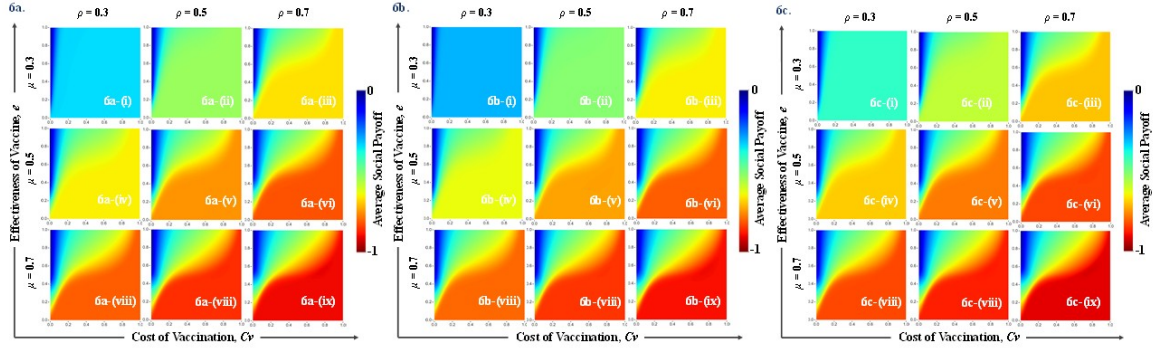


Figure 3.12: *Average Social Payoff (ASP) for distinct values of inoculation cost and effectiveness. Scenarios: 6a:  $\gamma = 0.18517$  ( $R_0 = 4.5$ ), 6b:  $\gamma = 0.27777$  ( $R_0 = 3.0$ ). 6c:  $\gamma = 0.33333$  ( $R_0 = 2.5$ ). Fixed parameters:  $\beta = 0.8333$ ,  $\delta = 0.38$ ,  $\alpha = 0.20$ ,  $q = 0.6$ ,  $i = 0.4$ . Rates of capture:  $\rho = 0.3, 0.5, 0.7$  and  $\mu = 0.3, 0.5, 0.7$ . Findings show that higher latent carrier ( $\rho$ ) and conveying ( $\mu$ ) rates influence ASP. Although ASP patterns resemble FES, differences across the critical line are notable. High isolation and quarantine rates yield higher ASP, illustrated by darker blue regions. This highlights the societal benefit of strong control measures.*

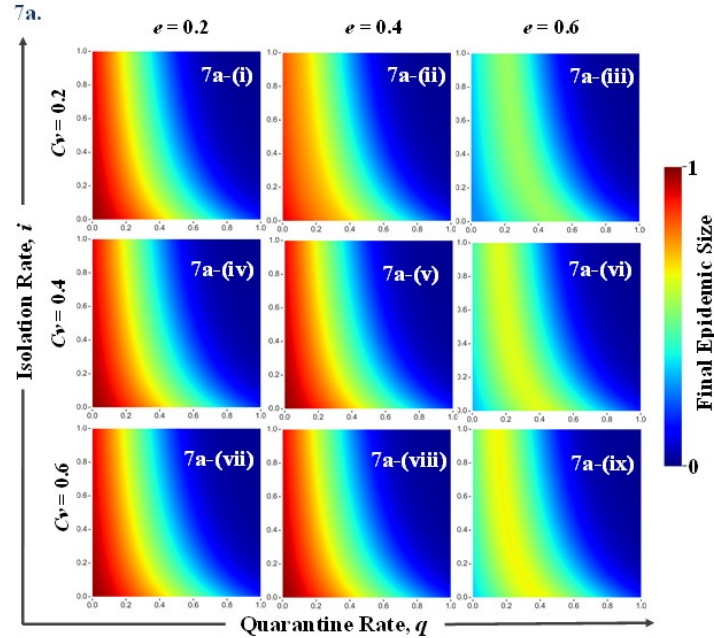


Figure 3.13: *Final Epidemic Size (FES) according to different isolation ( $i$ ) and quarantine ( $q$ ) rates for distinct combinations of immunization potency ( $e = 0.2, 0.4, 0.6$ ), and charge of the immunization ( $C_V = 0.2, 0.4, 0.6$ ). It is observed from the heat maps that a low quarantine/isolation rate leads to a higher epidemic intensity, which is denoted by dark red in the graphs. On the other hand, larger  $q$  and  $i$  values reduce the pandemic fitness, as evidenced by the darker blue lines. The 45 degree diagonal line represents the fair balance between the two control strategies.*

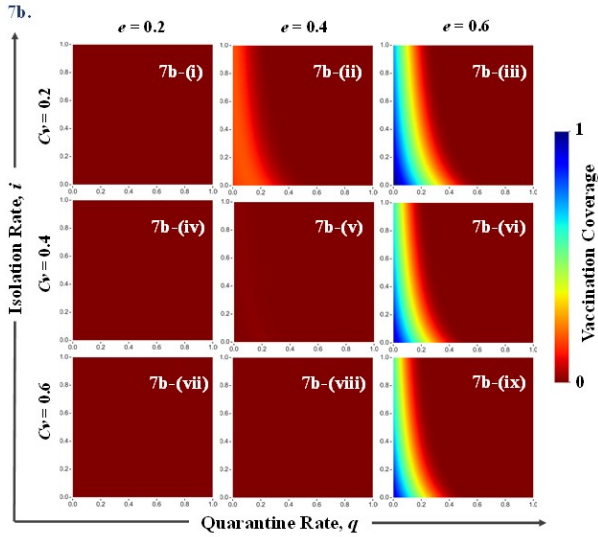


Figure 3.14: Vaccination Coverage ( $VC$ ) under different  $i$  and  $q$ , different  $e$ , and different  $C_v$  levels. Each panel corresponds to a specific pair of values for  $e$  and  $C_v$ . Low  $i$  and  $q$  bring about low vaccination coverage (dark red), whereas high  $i$  and  $q$  lead for high  $VC$  (dark blue). The 45 degree diagonal represents identical contributions from isolation and quarantine. Jets from red to blue denote growing vaccine coverage.

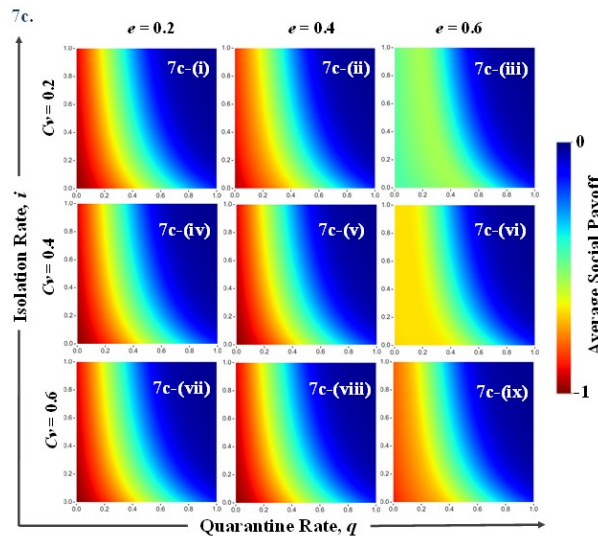


Figure 3.15: Average Social Payoff ( $ASP$ ) for varying  $i$  and  $q$  considering different  $e$  ( $e = \{0.2, 0.4, 0.6\}$ ) and  $C_v$  ( $C_v = \{0.2, 0.4, 0.6\}$ ) with the social distancing and quarantine rates. For each panel a different  $e$ - $C_v$  pair is considered. Low  $i$  and  $q$  decrease the  $ASP$  (red), but grows the society benefit (blue). Equal investment in quarantine and isolation is represented along the 45-degree diagonal. The red-to-blue shift is a symbol of the better societal progress.

## 4 Conclusion

In summary, our study examined two primary approaches to mitigate the risk of repeated pandemics and serious epidemics caused by contagious diseases: vaccination campaigns that are voluntary and enforced control (quarantine and social distancing). We thoroughly examined the advantages of social distancing (isolation) and quarantine rules for preventing illnesses using mathematical epidemiological and the concept of the immunization process. The complicated consequences of these techniques for control are comprehensively examined by our proposed model, which also assesses their applicability under different parametric settings to reduce the seriousness of infectious disease spread, especially in those who choose immunization as a preventative strategy. Nevertheless, given that vaccinations are only partially successful and that pandemic outbreaks happen often, longer-term approaches are needed to protect society as a whole in opposition against viruses. Our work's computational models highlight how crucial it is to implement these measures to halt the transmission of illness. In our proposed model, we add two parameters called latent carrier rate and conveying rate to observe the changes in the SVEIR model. If the values of these two parameters are increasing, the situation will worsen. Therefore, to mitigate the worsened situation, we need to build a strong controlling measure and these measures are quarantine and social distancing (isolation). We provide diagrams of phases for FES, VC, and ASP throughout our study to substantiate this assertion. Our framework effectively emphasizes the significance of both temporary securities in resolving community health concerns through the application of the IS-RA method modification rules and the mean-field estimate approach. It is evident from the computational models that regardless of places with extreme conditions, enforcing these strategies may improve the situation. We also demonstrate when and what in situations one policy is more effective than another and a variety of controls should be executed when the incidence of disease spreading is strong. A multi-layered defense against the transmission of illness is produced by combining many tactics, including contact tracking, immunization, hygiene habits, quarantine laws, and public health activities. Lastly, governments must put the safety of the people first when implementing each of these rules.

## Authors' contribution

Zarin Tusnim created the original draft, built the pictorial illustrations, conducted the numerical simulations to validate the suggested model, and built the model. Muntasir Alam assisted to reviewing and editing the manuscript, analyzed the results. He also oversaw the project as a whole.

## Declaration of competing interest

There are no disclosed conflicts of interest for the writers. We make it clear the submission is unique and not being considered by another publication.

## Data sharing

Regarding the current research, no data is currently available. Since our work follows a theoretical and mathematical framework, we neither create nor analyze any data sets.

## Ethical approval

The manuscript can be published without consent. All authors have approved for publication and Each author has consulted to publication and accepted the responsibility work done.

## References

- [1] M. A. Amarala and M. M. de Oliveira, “An epidemiological model with voluntary quarantine strategies governed by evolutionary game dynamics,” *Chaos, Solitons Fractals*, pp. 2–14, 2021.
- [2] C. Castillo-Chavez *et al.*, “Mathematical models of isolation and quarantine,” *American Medical Association*, vol. 290, pp. 2876–2877, 2003.

- [3] Q. Z. Y. Huang, “Game-theoretic frameworks for epidemic spreading and human decision-making: A review,” *Dynamic Games and Applications*, vol. 12, pp. 7–48, 2022.
- [4] K. M. A. Kabir, “How evolutionary game could solve the human vaccine dilemma,” *Chaos, Solitons Fractals*, pp. 1–25, 2021.
- [5] Y. N. K. Agaba *et al.*, “Dynamics of vaccination in a time delayed epidemic model with awareness,” *Mathematical Biosciences*, vol. 294, pp. 92–99, 2017.
- [6] S. Bhattacharyya and C. T. Bauch, “Evolutionary game theory and social learning can determine how vaccine scares unfold,” *PLoS Computational Biology*, pp. 1–14, 2012.
- [7] M. A. Habib, K. M. A. Kabir, and J. Tanimoto, “Do humans play according to the game theory when facing the social dilemma situation? a survey study,” *Evergreen*, vol. 07, no. 01, pp. 1–9, 2020.
- [8] V. K. Yadav and J. P. Yadav, “Cognizance on pandemic corona virus infectious disease (covid-19) by using statistical technique: A study and analysis,” *Evergreen*, pp. 329–334, 2020.
- [9] E. Boros, V. Gurvich, and P. G. Franciosa, “Deterministic person shortest path and terminal games on symmetric digraphs have nash equilibria in pure stationary strategies,” *International Journal of Game Theory*, pp. 2–26, 2023.
- [10] K. M. A. Kabir and J. Tanimoto, “The role of advanced and late provisions in a co-evolutionary epidemic game model for assessing the social triple-dilemma aspect,” *Journal of Theoretical Biology*, pp. 1–32, 2020.
- [11] D. I. Rice, L. W. Fu, M. A. Nowak, and N. F. Fu, “Imitation dynamics of vaccination behaviour on social networks,” *Proceedings of the Royal Society B: Biological Sciences*, vol. 278, pp. 42–49, 2011.
- [12] M. T. Alam *et al.*, “A game theoretic approach to discuss the positive secondary effect of vaccination scheme in an infinite and well-mixed population,” *Chaos, Solitons Fractals*, vol. 125, pp. 201–213, 2013.
- [13] H. W. Hethcote *et al.*, “Effects of quarantine in six endemic models for infectious diseases,” *Mathematical Biosciences*, vol. 180, pp. 141–160, 2002.
- [14] A. Giubilini *et al.*, “Quarantine, isolation and the duty of easy rescue in public health,” *Developing World Bioethics*, vol. 18, pp. 182–189, 2017.
- [15] M. S. U. K. M. A. Kabir, “Coupled simultaneous analysis of vaccine and self-awareness strategies on evolutionary dilemma aspect with various immunity,” *Helijon*, pp. 1–37, 2023.
- [16] M. Alam, K. M. A. Kabir, and J. Tanimoto, “Based on mathematical epidemiology and evolutionary game theory, which is more effective: quarantine or isolation policy?” *Journal of Statistical Mechanics: Theory and Experiment*, pp. 1–27, 2020.
- [17] D. Z. Wang *et al.*, “Evolutionary game of digital decision-making in supply chains based on system dynamics,” *RAIRO Operations Research*, vol. 58, pp. 475–510, 2024.
- [18] J. Tanimoto, *Evolutionary Games with Sociophysics Analysis of Traffic Flow and Epidemics*. US: Springer, 2018.
- [19] M. K. J. T. Muntasir Alam, Sumaiya Jamila, “Assessing the trade-off between voluntary and forced interventions to control the emergence of recurring pandemics—an evolutionary game-theoretic modeling,” *Scientific Research*, vol. 13, no. 03, March, 2025.
- [20] M. K. Mansura Akter, Muntasir Alam, “An in-silico game theoretic approach for health intervention efficacy assessment,” *ScienceDirect*, vol. 5, June, 2024.
- [21] M. K. Umma Kulsum, Muntasir Alam, “Modeling and investigating the dilemma of early and delayed vaccination driven by the dynamics of imitation and aspiration,” *ScienceDirect*, vol. 178, January, 2024.
- [22] M. K. Shobha Islam, Md. Shahidul Islam, “Effectiveness of bed nets and media awareness in dengue control: A fuzzy analysis,” *ScienceDirect*, vol. 20, September, 2025.

- [23] T. Reluga, “An sis epidemiology game with two subpopulations,” *Journal of Biological Dynamics*, vol. 3, pp. 515–531, 2009.
- [24] J. Iwamura, J. Tanimoto, and F. Yamauchi, “Effect of intermediate defense measures in voluntary vaccination games,” *Journal of Statistical Mechanics: Theory and Experiment*, p. P02008, 2016.
- [25] K. M. A. Kabir and J. Tanimoto, “Dynamical behaviors for vaccination can suppress infectious disease—a game theoretical approach,” *Chaos, Solitons Fractals*, vol. 123, pp. 229–239, 2019.
- [26] A. B. Gumel *et al.*, “Modeling the impact of quarantine during an outbreak of ebola virus disease,” *Infectious Disease Modelling*, vol. 4, pp. 12–27, 2019.
- [27] O. Cliff, C. M. Peak, Q. Johnson, V. K. Yadav *et al.*, “Network properties of salmonella epidemics,” *Scientific Reports*, vol. 9, pp. 1–6, 2019.
- [28] H. Gintis, “Classical versus evolutionary game theory,” *Journal of Consciousness Studies*, vol. 1-2, pp. 300–304, 2000.
- [29] M. A. Nowak and K. Sigmund, “Evolutionary dynamics of biological games,” *Science*, vol. 303, pp. 793–799, 2004.
- [30] T. Fujimoto and Y. Aruka, *Evolutionary Game with Sociophysics*. Tokyo, 2004.
- [31] J. Tanimoto, *Fundamentals of evolutionary game theory and its applications*. Springer, 2015.
- [32] K. K. Alam and J. Tanimoto, “Three-strategy and four-strategy model of vaccination game introducing an intermediate protecting measure,” *Applied Mathematics and Computation*, vol. 346, pp. 408–422, 2019.
- [33] J. T. Kuga and K. Kugaa, “Impact of imperfect vaccination and defense against contagion on vaccination behavior in complex networks,” *Journal of Statistical Mechanics: Theory and Experiment*, pp. 1–25, 2018.
- [34] J. Tanimoto and M. J. K. Kuga, “To vaccinate or not to vaccinate: a comprehensive study of vaccination-subsidizing policies with multi-agent simulations and mean-field modeling,” *Journal of Theoretical Biology*, vol. 469, pp. 107–126, 2019.
- [35] K. M. A. Kabir, M. S. Islam, and M. S. Ullah, “Understanding the impact of vaccination and self-defense measures on epidemic dynamics using an embedded optimization and evolutionary game theory methodology,” *Vaccines*, vol. 11, 2023.
- [36] B. Shi *et al.*, “Voluntary vaccination through self organizing behaviours on locally mixed social networks,” *Scientific Reports*, vol. 7, pp. 1–11, 2017.
- [37] K. M. A. Kabir and J. Tanimoto, “Effect of information spreading to suppress the disease contagion on the epidemic vaccination game,” *Chaos, Solitons Fractals*, pp. 2–14, 2019.
- [38] C.-R. Cai, Z.-X. Wu, and J.-Y. Guan, “Behavior of susceptible-vaccinated–infected–recovered epidemics with diversity in the infection rate of individuals,” *Physical Review E*, vol. 88, 2013.
- [39] E. Fujimoto and J. Tanimoto, “Impact of stubborn individuals on a spread of infectious disease under voluntary vaccination policy,” pp. 816–858, 2015.
- [40] A. Traulsen, D. Semmann, R. D. Sommerfeld, H.-J. Krambeck, and M. Milinski, “Human strategy updating in evolutionary games,” *Proceedings of the National Academy of Sciences*, pp. 1–6, 2010.
- [41] J. O. Lloyd-Smith, S. J. Schreiber, P. E. Kopp, and W. M. Getz, “Curtailing transmission of severe acute respiratory syndrome within a community and its hospital,” *Proceedings of the Royal Society B*, vol. 270, pp. 1979–1989, 2003.
- [42] K. T. D. Eames and M. J. Keeling, “Networks and epidemic models,” *Journal of the Royal Society Interface*, vol. 2, pp. 295–307, 2005.
- [43] K. Kuga and J. Tanimoto, “Which is more effective for suppressing an infectious disease: imperfect vaccination or defense against contagion?” *Journal of Statistical Mechanics: Theory and Experiment*, pp. 2–15, 2018.